Materials Science-Poland, *Vol. 26*, *No. 3*, *2008*

Surface microstructure and specific surface area of pure and Na-substituted gyrolites

K. BALTAKYS[1*], R. SIAUCIUNAS[1], S. KITRYS[2]

[1]Department of Silicate Technology, Kaunas University of Technology, Radvilenu 19, LT – 50270 Kaunas, Lithuania

[2]Department of Physical Chemistry, Kaunas University of Technology, Radvilenu 19, LT – 50270 Kaunas, Lithuania

Pure gyrolite was synthesized within 32 h at 200 °C from a stoichiometric composition (the molar ratio CaO/SiO_2 was equal to 0.66 with water/solid ratio of the suspension equal to 10.0) of the initial CaO and $SiO_2 \cdot nH_2O$ mixture. Meanwhile, Na-substituted gyrolite was synthesized twice quicker – within 16 h at 200 °C. These compounds were characterized by XRD, STA, FT-IR, SEM/EDS and BET analysis. It was found that gyrolite is a mesoporous material. Its specific surface area S_{BET} = 143.15 m^2/g, the radius of dominant plate pores r_p = 80–90 Å, the calculated total pore volume ΣV_p = 0.661 cm^3/g. Gyrolite texture changes upon introducing Na^+ ions into its crystal structure: the specific surface area S_{BET} diminishes to 27.24 m^2/g, the radius of dominant cylindric pores r_p = 60–70 Å, the calculated total pore volume ΣV_p = 0.118 cm^3/g.

Key words: *gyrolite; Na-substituted gyrolite; pore size;* BET *equation*

1. Introduction

Calcium silicate hydrates are highly multiplex systems with over 30 stable phases. From a theoretical and practical points of view, the synthesis, properties and structure of the main calcium silicate hydrates (C–S–H(I), 1.13 nm tobermorite, xonotlite, α-C_2S hydrate and gyrolite have been analyzed in detail [1–16]. Majority of these compounds occur naturally or may be synthesized in the laboratory.

Recently, the interest in gyrolite has increased because of new possibilities of its application: it may be used to educe heavy metal ions and remove them from wastewaters [17]. Of specific interest is the purported ability of gyrolite to separate supercoiled plasmid, opencircular plasmid, and genomic DNA [18].

*Corresponding author, e-mail: kestutis.baltakys@ktu.lt

The structure, optical properties and chemistry of natural gyrolite were studied by Mackay and Taylor [19], Chalmers et al. [20], Gard et al. [21], Lachowski et al. [22], and others [23, 24]. However, their opinions differ. A full structural solution for gyrolite was proposed by Merlino [25]. Currently it is supposed that his proposed model of gyrolite crystal lattice precisely represents a real structure of this compound. Merlino showed that this phase structure is built up by the stacking of SiO_4 tetrahedral sheets (S_1, S_2, and $\overline{S}_2$, where S_2 and $\overline{S}_2$ are symmetry-related units) and CaO_6 octahedral sheets (O and $\overline{O}$, which are symmetry-related units). The $Si–O_4$ tetrahedra in the silicate sheets are linked by sharing three oxygen atoms to give a pseudo-hexagonal sheet structure with tetrahedral in six-membered rings. Each unit cell contains three distinct silicate sheets two of which (S_2 and $\overline{S}_2$) are symmetrically equivalent with the six-membered rings having four tetrahedra pointing one way and two the other; the third sheet (S_1) has alternate tetrahedral six-membered rings pointing in opposite directions. These sheets are linked by layers of Ca–(O, OH) polyhedra to build up a "complex layer" perpendicular to the *c* axis. The stacked complex layers ($\overline{S}_2$, $\overline{O}$, S_1OS_2) with composition $[Ca_7Si_{12}O_{30}(OH)_4]^{2-}$ are connected through interlayer sheets made by Ca^{2+} ions and water molecules (Fig. 1).

However, some properties (like sorption capacity) depend not only on the crystal lattice of the porous body but also on the surface microstructure and specific surface area, as well as dominant pore size and their differential distribution according to the radius in the compound. In the case of gyrolite crystal lattice, those properties usually depend on the proportion of crystalline (S_1, S_2, $\overline{S}_2$) and amorphous (X sheet) parts (Fig. 1). However, data presented in references about the texture of low-base compounds (C/S = 0.6–0.8) are not extensive and often controversial.

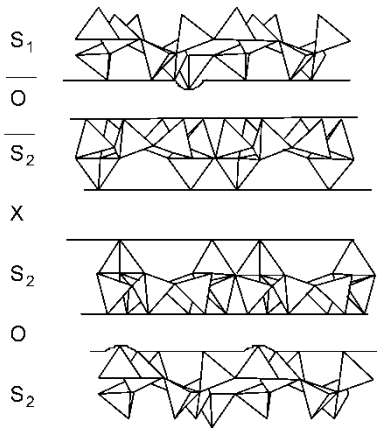

Fig. 1. Schematic drawing of the crystal structure of gyrolite as viewed along the *a* direction

The aim of this paper is to determine the gyrolite surface microstructure and specific surface area, as well as the dominant pore sizes and their differential distribution

according to the radius in this compound, crystal size and form, stability at low and high temperature and the influence of Na^+ ions on these properties.

2. Materials and methods

The following reagents were used as starting materials: fine-grained $SiO_2 \cdot nH_2O$ (Reachim, Russia, ignition losses 21.43%, specific surface area S_a = 1560 m²/kg by Blaine's); NaOH solutions (Reachim, Russia; c = 1.04 %); CaO (99.6 % Reachim, Russia) additionally was burned at 1000 ºC for 0.5 h.

The synthesis of gyrolite has been carried out in unstirred suspensions in vessels of stainless steel. Pure gyrolite was synthesized within 32 h at 200 °C from a stoichiometric composition (the molar ratio of CaO/SiO_2 was equal to 0.66 with water/solid ratio of the suspension equal to 10.0) of the initial CaO and $SiO_2 \cdot nH_2O$ mixture. Na-substituted gyrolite was synthesized within 16 h at 200 °C. The amount of NaOH, corresponding to 5% of Na_2O from the mass of dry materials, was added in the form of solution and additionally an appropriate quantity of water was added that water/solid ratio of the suspension kept equal to 10.0. These conditions of the syntheses were chosen according to previously published data [16]. The products of the syntheses were filtered, rinsed with ethyl alcohol to prevent carbonization of materials, dried at 50 ± 5 ºC and sieved through a sieve with a mesh width of 50 μm.

The specific surface area of the raw materials was determined by the Blaine's method with an air permeability apparatus (Model 7201, Toni Technik Baustoffprüfsysteme GmbH).

The X-ray powder diffraction data were collected with a DRON–6 X-ray diffractometer in the Bragg–Brentano geometry using Ni-filtered CuK_α radiation and a graphite monochromator, operating at 30 kV and emission current of 20 mA. The step-scan covered the angular range 2–60° (2θ) in steps of 2θ = 0.02°. The computer program X-fit [26] was used for diffraction profile refinement under the pseudoVoid function and for the description of the diffractional background under the 3rd degree of the Tchebyshev polynom.

Simultaneous thermal analysis (STA) (differential scanning calorimetry DSC and thermogravimetry (TG)) was carried out on a Netzsch instrument STA 409 PC at the heating rate of 15 °C/min, in the temperature range from 30 °C up to 1000 °C under an air atmosphere. The ceramic sample handlers and crucibles of Pt-Rh were used.

Scanning electron microscopy (SEM) (Oxford ISIS Leo 440 i) coupled with energy dispersive X-ray spectrometer (EDS) was performed using an accelerating voltage of 20 kV and a working distance of 10 mm for SEM observations and a 200 s accumulation time for EDS analyses.

FT-IR spectra have been carried out with a Perkin Elmer FT–IR Spectrum X system. Specimens were prepared by mixing 1 mg of the sample with 200 mg of KBr. The spectral analysis was performed in the range of 4000–400 cm^{-1} with the spectral

resolution of 1 cm^{-1}. The surface areas, total pore volumes and pore size distributions of the products of the syntheses were performed by a BET surface area analyzer "Quantasorb" (Quantachrome).

The specific surface area of gyrolite was calculated by the BET equation using the data of the lower part of N_2 adsorption isotherm ($0.05 < p/p_0 < 0.35$):

$$\frac{1}{X\left(\frac{p_0}{p}-1\right)} = \frac{C-1}{X_m C}\cdot\frac{p}{p_0}+\frac{1}{X_m C}$$

where X is the mass of adsorbate, adsorbed on the sample at relative pressure p/p_0, p – the partial pressure of adsorbate, p_0 – the saturated vapour pressure of adsorbate, X_m – the mass of adsorbate adsorbed at a coverage of one monolayer, C is a constant which is a function of the heat of the adsorbate condensation and heat of adsorption.

The BET equation yields a straight line when $1/X[(p_0/p) - 1]$ is plotted versus p/p_0. The slope of $(C - 1)/X_mC$ and the intercept of $1/X_mC$ was used to determine X_m and C: slope $S = (C - 1)/X_mC$ and intercept $I = 1/X_mC$. Solving for X_m yields $X_m = 1/(S + I)$. BET plot is usually found to be linear in the range $p/p_0 = 0.05$–0.35. The total surface area of the sample S_t was determined from the equation $S_t = X_m N A_{cs}/M$, where M is the molecular mass of the adsorbate, N – Avogadro's constant, A_{cs} – the cross-sectional area occupied by each nitrogen molecule (16.2×10^{-20} m^2). The specific surface area was given by the equation $S_{BET} = S_t/m$, where m is the mass of gyrolite sample. The total pore volumes and pore size distributions were calculated according to the corrected Kelvin equation and Orr et al. scheme [27, 28] based on the entire N_2 desorption isotherm at 77 K. The Kelvin equation relates the depression of the adsorbate vapour pressure to the radius of a capillary filled with adsorbate:

$$\ln\frac{p}{p_0} = -2\,\frac{\gamma\, V_m \cos\theta}{R\, T\, r_k}$$

where p is the saturated vapour pressure in equilibrium with the adsorbate condensed in a capillary or a pore, p_0 – the normal adsorbate saturated vapour pressure, γ – the surface tension of nitrogen at its boiling point, V_m – the molar volume of liquid nitrogen, θ – the wetting angle (usually taken 0° hence $\cos\theta = 1$), R – the gas constant, T – the absolute temperature, and r_K the Kelvin radius of pore. When N_2 is used as the adsorbate, the Kelvin equation can be rearranged

$$r_k = \frac{4.146}{\lg\frac{p_0}{p}}$$

The Kelvin radius r_K is not the actual pore radius because some adsorption takes place on the wall of the pore prior to the occurrence of condensation in the pore. During desorption, an adsorbed layer remains on the wall when evaporation takes place.

Therefore, the true pore radius r_p was calculated from the equation $r_p = r_K + t$, where t is the thickness of the adsorbed layer, calculated according to the Halsey equation [27]:

$$t = 3.54\left[\frac{5}{\ln\frac{p_0}{p}}\right]^{1/3}$$

where 3.54 is the thickness of one adsorbed nitrogen layer. If the pores are assumed to be cylindrical and if the relative pressure is changed from $(p/p_0)_2$ to $(p/p_0)_1$, the pores between radii r_2 and r_1 will empty ($p_2 < p_1$, $r_2 < r_1$). When p_2 is lowered to p_1, the thickness of the adsorbed film on previously emptied pores changes from t_2 to t_1. The volume of liquid (V_L) evaporated due to emptying of pores and the decrease in thickness of adsorbed layers in previously empty pores was calculated by the following equation:

$$V_L = \pi\left(\overline{r}_p - t_2\right)^2 L + (t_2 - t_1)\sum A$$

where $\overline{r}_p$ is the average pore radius in the interval r_2 to r_1, L – the total length of all pores in the range from r_2 to r_1, A – the area of adsorbed film remaining in the pores after the evaporation out of the pores has occurred. The mean volume of pores with $\overline{r}_p$ is $V_p = \pi\overline{r}_p^2 L$. Then

$$V_p = \left(\frac{\overline{r}_p}{\overline{r}_p - t_2}\right)^2 V_L - \left(\frac{\overline{r}_p}{\overline{r}_p - t_2}\right)^2 (t_2 - t_1)\sum A$$

substituting $r_p = r_K + t$:

$$V_p = \left(\frac{\overline{r}_p}{\overline{r}_K}\right)^2 \left(V_L - \Delta t\sum A\right)$$

The volume of liquid desorbed in any interval of desorption isotherm is related to the volume of gas by the equation: ΔV_L (cm^3) = $\Delta V_{gas}(1.54 \times 10^{-3})$. For cylinders, A is given by

$$A = \frac{2\Delta V_p}{\overline{r}_p} \times 10^4 \quad [\mathrm{m}^2]$$

with V_p in cm^3 and r_p in Å.

The analysis of the desorption isotherms was completed when ($\Delta t\Sigma A$) exceeded ΔV_L because the desorbed gas originates from the adsorbed layer rather than from

evaporation of the liquid from inside the pores. ΣA is the cumulative surface area and is obtained by summing A in each radius interval.

The shapes of natural pores are usually non-uniform. Their complicated shapes for calculation purposes are usually approximated by selected geometrical models. Among many models (slit-like, ink-bottle, conical, globular, etc.) the most frequently used is the cylindrical pore model. Moreover, gyrolite has a plate-like crystal structure. It is thus conceivable that slit-like (plates) pores will dominate in the gyrolite crystal lattice. For the calculations of slit-like pores we used the following equation:

$$\bar{d}_p = r_K + 2t; \qquad V_p = \frac{\bar{d}_p}{r_K}\left(\Delta V_L - 2\Delta t \sum A\right); \qquad A = \frac{2V_p}{d_p}$$

where $\bar{d}_p$ is the distance between two plates (in Å).

3. Results and discussion

Our preliminary investigation focused on the synthesis and characterization of pure gyrolite (without any additives) and Na-substituted gyrolite. The results of XRD

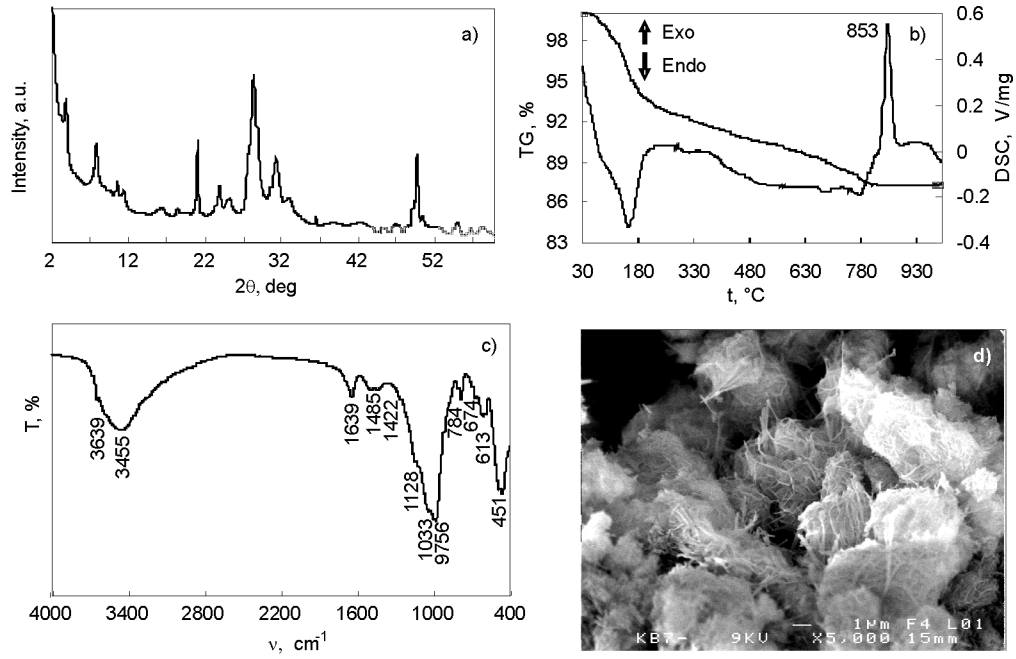

Fig. 2. X-ray diffraction pattern (a), DSC–TG curve (b), FT-IR spectrum (c) and SEM micrograph (d) of pure gyrolite. Duration of the hydrothermal synthesis at 200 °C equals 32 h

studies confirmed that in the $CaO–SiO_2 \cdot nH_2O–H_2O$ system within 32 h at 200 °C pure gyrolite was formed, whereas in the samples doped with 5% Na_2O within 16 h at 200 °C only Na-substituted gyrolite was found. An intensive peak with the *d* spacing of 2.2 nm is attributed to gyrolite, i.e. this diffraction reflection is not characteristic of other calcium silicate hydrates. Moreover, in the X-ray diffraction pattern, the peaks which are also typical of gyrolite have been identified (*d* spacings – 1.1262; 0.8371; 0.4197; 0.3732; 0.3511; 0.2803; 0.2141 nm, Fig. 2a). It should be noted that the mentioned properties of gyrolite are slightly altered by Na^+ ions inserted into crystal lattice of the former compound: the main basal reflection *d* spacing increases to 2.324 nm in X-ray diffraction pattern (Fig. 3a).

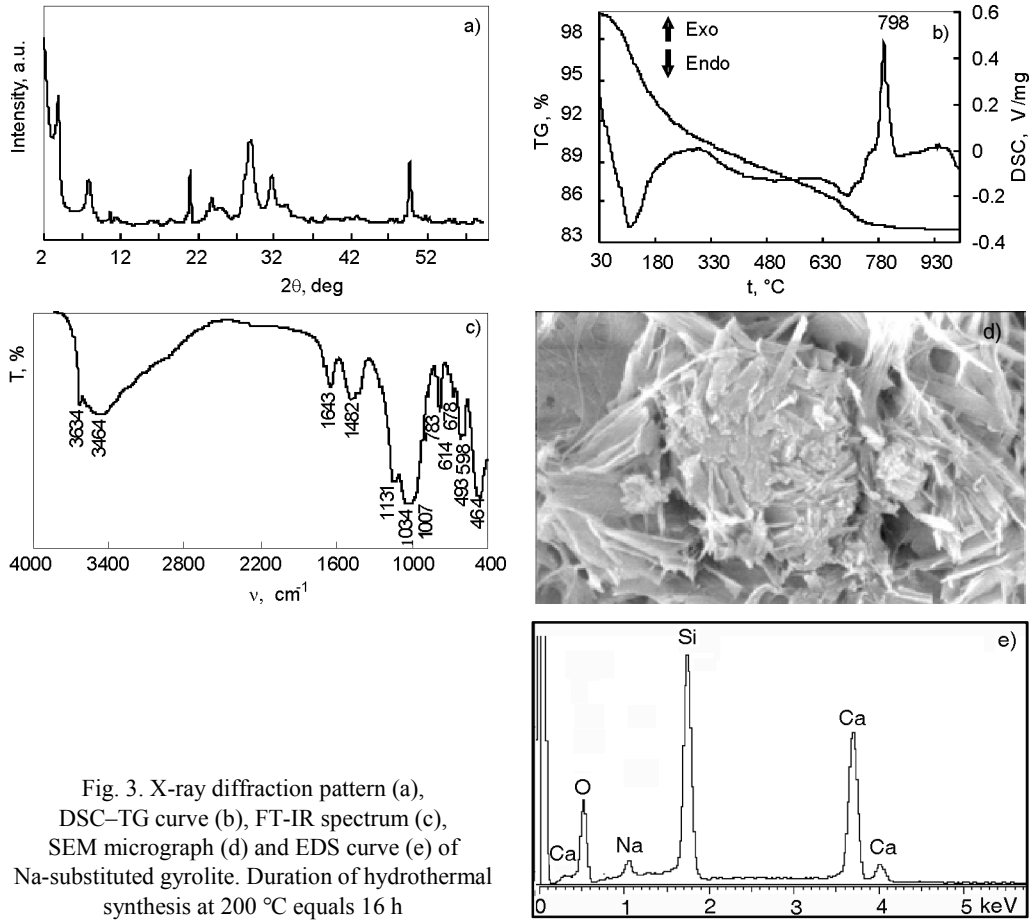

Fig. 3. X-ray diffraction pattern (a), DSC–TG curve (b), FT-IR spectrum (c), SEM micrograph (d) and EDS curve (e) of Na-substituted gyrolite. Duration of hydrothermal synthesis at 200 °C equals 16 h

On the DSC curve, only two thermal effects corresponding to gyrolite are visible. A broad endothermic peak appearing in the temperature range of 137–143 °C is related to the loss of physisorbed and interlayer water from the crystal structure of gyrolite. The other exothermic peak is associated with recrystallization of this compound

into wollastonite (Fig. 2b). This step is accompanied by a complete destruction of the gyrolite structure. In the case of Na-substituted gyrolite, in DSC curve the shape of wollastonite formation peak changes and moves to lower temperature (Fig. 3b, exothermic peak at 798 °C). The findings of SEM also confirmed the formation of gyrolite in the synthesis products. The SEM photos show that plate Na-substituted gyrolite crystals are much larger than those of pure gyrolite (Figs. 2d, 3d). EDS analysis proved the presence of sodium (~ 3 %) in the crystal structure of gyrolite (Fig. 3e). All of these findings have been confirmed by the FT-IR spectroscopy data, which can be used to distinguish gyrolite from other calcium silicate hydrates [29]. A sharp peak near 3635 cm^{-1} is visible only in the gyrolite spectrum (Figs. 2c, 3c). Its presence proves that clearly distinguished OH positions exist in the structure of gyrolite connected only with Ca atoms and not influenced by hydrogen bridge links. A wide band near 3446 cm^{-1} means the opposite –molecular water forms hydrogen bridge links in the interlayers. The bands in the range of 1634 cm^{-1} are assigned to $\delta(H_2O)$ vibrations and confirm this presumption. Vibrational modes for gyrolite and Na-substituted gyrolite are presented in the Table 1.

Table 1. Vibrational modes for gyrolite and Na-substituted gyrolite

Bend assigment	Band position (wavenumber), cm^{-1}	
	Gyrolite	Na-substituted gyrolite
δ(O–Si–O)	451	464
	492	493
δ(Si–O–Si)	596	598
ν(OH–)?	613	614
ν_s(Si–O–Si)	674	678
	784	783
ν(O–Si–)	975	
ν_{as}(Si–O–Si) from Q^3	1033	1007
	1128	1034
		1131
$\nu(C–O_3^{2-})$	1422	1482
	1485	
δH_2O(bending)	1639	1643
ν(OH^-)	3455	3464
	3639	3634

To evaluate the stability of gyrolite structure at low temperatures and to estimate the influence of the adsorbed water vapour (adsorbate) on the structure of its crystal lattice, gyrolite samples were saturated with water vapour, i.e. kept in desiccator for 60 h under various relative pressures (p/p_0 = 1; 0.877; 0.753; 0.56; 0.355). Then each sample was frozen in liquid nitrogen (–197 °C) for 15 min and then heated to room temperature (20 °C). X-ray diffraction patterns obtained after these experiments show that there was essentially no change in the structure of gyrolite (Fig. 4).

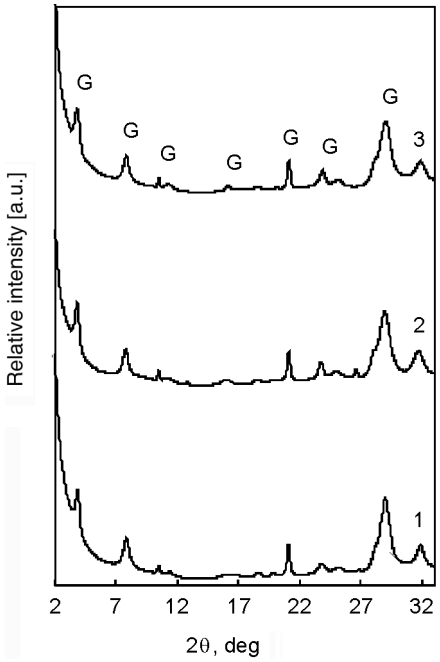

Fig. 4. X-ray diffraction patterns of gyrolite subject to water vapour adsorption: 1 – pure gyrolite; 2 – saturated (60 h) with water vapour under $p/p_0 = 1$; 3 – saturated (60 h) with water vapour under $p/p_0 = 1$, frozen in liquid nitrogen (–197 °C) during 15 min and heated to room temperature; G – gyrolite

Therefore, it can be stated that a stable monomolecular layer of adsorbed N_2 is formed on the surface of the gyrolite pores, and the calculations of the specific surface are reliable. The line prominence ratios R^2 are equal to 0.9866 for gyrolite and 0.9969 for Na-substituted gyrolite (Table 2).

Table 2. Parameters of the BET equation of gyrolite and Na-substituted gyrolite

Adsorbent	Parameters of BET equation		X_m, g	S_{BET}, m^2/g	C_{BET}	R^2
	S	I				
Gyrolite	4117.4	6.54	0.00024	143.15	637	0.987
Na-substituted gyrolite	8136.8	6.20	0.00012	27.24	1034	0.997

S_{BET} significantly decreases after introducing Na^+ ions into the crystal lattice of gyrolite. It equals 143.15 m^2/g, and diminishes to 27.24 m^2/g after 5% of Na_2O has been added to primary mixtures. These findings once more prove the influence of Na^+ ions on the synthesis processes of gyrolite when bigger particles are formed and at the same time the specific surface area decreases.

The value of C_{BET} constant proves that the structure of gyrolite crystals consists of disorder sheets (gel inserts, i.e., it has no firm frame). It is already known that C_{BET} values range from 50 to 200, higher values indicating a possibility of chemisorption of N_2 at 77 K or an unstable structure of the analysed materials. The highest $C_{BET} = 1034$ was obtained when Na^+ ions were introduced into the gyrolite structure. The volume of gyrolite pores and distribution of their radii were calculated based on the isotherms

of N_2 adsorption–desorption (Figs. 5, 6). The isotherms are characteristic of mesopore materials. Isotherms have a clear bend (point A). Micropore sorbents do not have a point A in the $0.05 \le p/p_0 \le 0.30$ range. A characteristic feature of the isotherms in gyrolite is hysteresis: desorption curves in Fig. 5 are shifted "to the left" with respect to the adsorption isotherms. This is characteristic of mesopore solid bodies when diameters of pores vary from 15 to 500 Å.

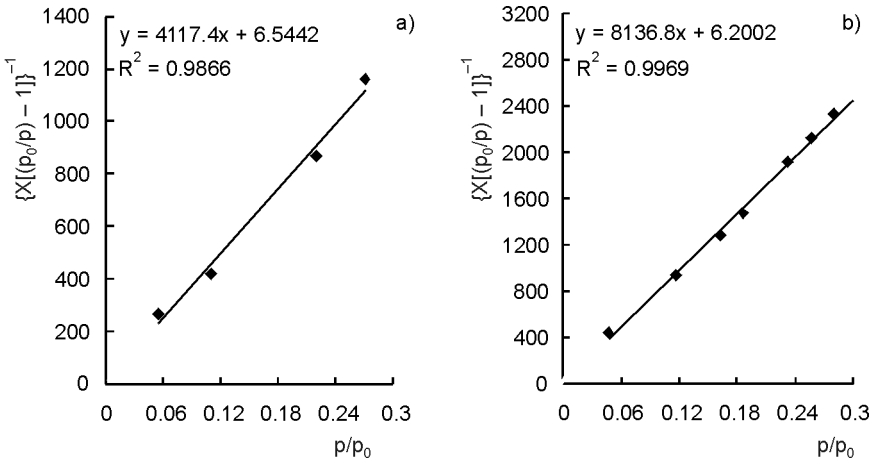

Fig. 5. BET isotherms of N_2 adsorption of gyrolite (a) and Na-substituted gyrolite (b) at 77 K

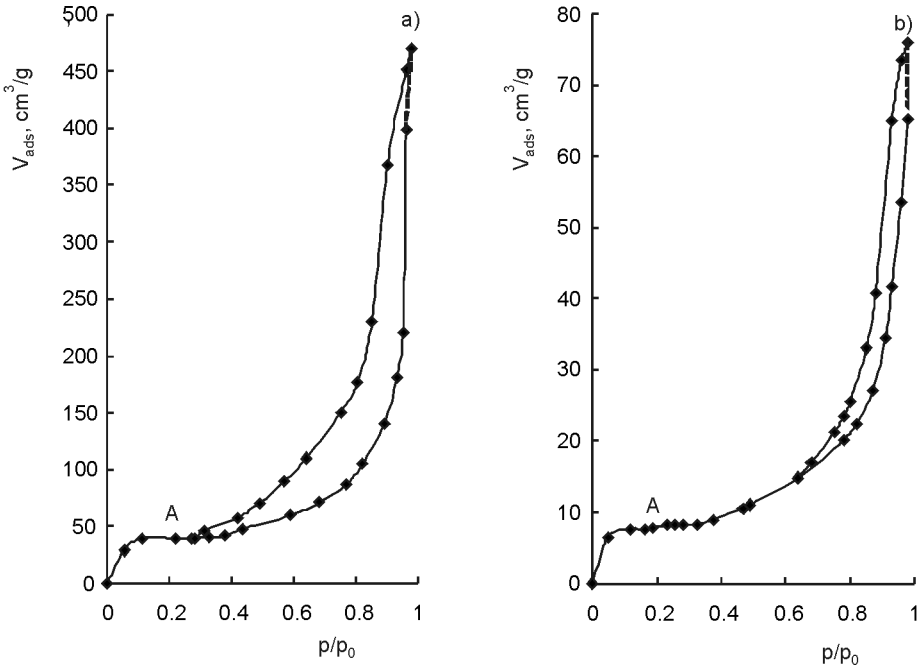

Fig. 6. Isotherms of N_2 adsorption–desorption of gyrolite (a) and Na-substituted gyrolite (b) at 77 K

According to the IUPAC classification, isotherms of pure gyrolite correspond to the case when pores are formed between parallel crystal plates (H3 type), adsorption and desorption coincide in the area of low p/p_0 amounting to about 0.30 and the isotherm of desorption has a refraction. And, on the contrary, after introducing Na^+ ions, the isotherm of hysteresis becomes characteristic of pores having a cylindrical or open tubular form. In this case, adsorption and desorption coincide in the area of $p/p_0 \approx 0.70$ and the hysteresis is narrow. It can be cautiously assumed that Na^+ ions are spread between the silicate layers of the crystal lattice of gyrolite. A possible formation of hydrogen bridge links in the X-interlayer of Na-substituted gyrolite structure is presented in Fig. 7.

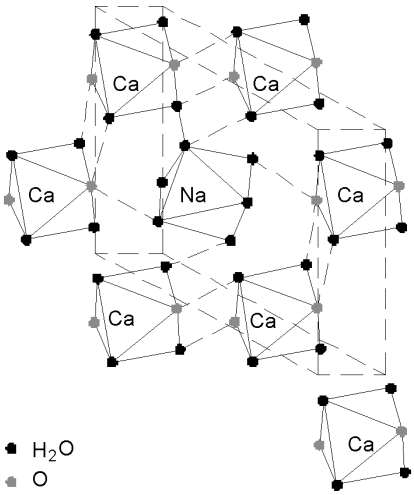

Fig. 7. Formation of hydrogen bridge links in the X-interlayer of Na-substituted gyrolite structure

The distribution of pore diameters is calculated according to the common model of a dominating form of pores. The most suitable model of pore distribution is the one whose experimentally defined S_{BET} value is the closest to the value of the calculated specific surface ΣA. Therefore, the distribution of pores to the diameters was calculated according to two models (cylindrical pores and pores between parallel plates). To calculate the distribution of pores of the pure gyrolite to the diameters the most suitable model is when pores are formed of parallel pores (the measured $S_{BET} = 143.15$ m^2/g, the calculated $\Sigma A = 157.71$ m^2/g). In this case, S_{BET} and ΣA differ by only 9.23%. In the case of cylindrical pore model S_{BET} and ΣA differed by over than 52.57%.

It is accepted that the model is the right one when this difference does not exceed 20% (compare $S_{BET} = 143.15$ m^2/g, and $\Sigma A = 272.77$ m^2/g). The dominating pores of the pure gyrolite are of about 8–9 nm in diameter, the total pore volume ΣV_p is 0.661 cm^3/g. Meanwhile, the more suitable model of cylindrical pores is for Na-substituted gyrolite because the measured $S_{BET} = 27.24$ m^2/g, and the calculated $\Sigma A = 30.25$ m^2/g. In this case, the diameters of the dominating pores are ranging from 6 to 7 nm, and the pore volume significantly decreases compared to the pure gyrolite and equals 0.12 cm^3/g.

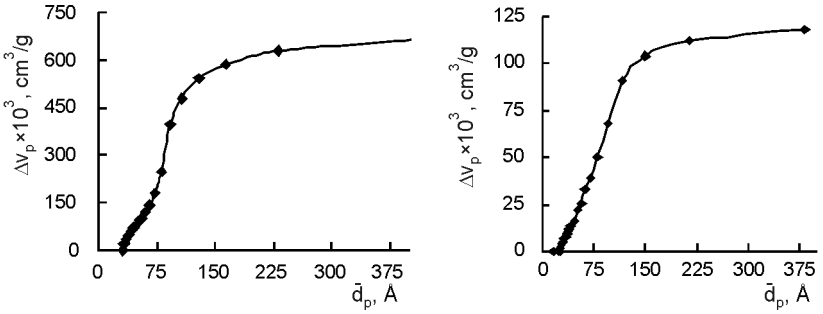

Fig. 8. Total pore volumes of gyrolite (a) and Na-substituted gyrolite (b)

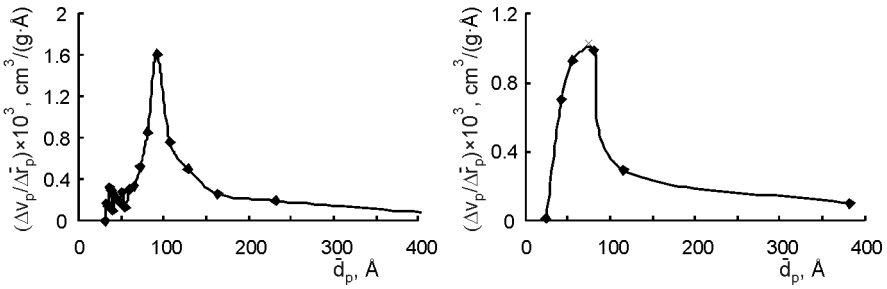

Fig. 9. Differential distributions of volume pore sizes of gyrolite (a) and Na-substituted gyrolite (b)

The results of the analysis of the specific surface confirmed the data obtained by other researchers [30]. Nocun-Wczelik also states that gyrolite is a mesopore compound and its S_{BET} varies depending on the synthesis conditions, additions used, etc. Thus, pure gyrolite satisfies the main requirements for adsorbents (i.e., high specific surface, smoothness, particles of a proper size, mechanical resistance to high pressure) and can be used as an adsorbent and/or chemisorbent. Besides, addition of Na_2O to the primary mixture allows one to alter the size of the particles, the specific surface area, the total pore volume, the differential pore distribution to the radii.

4. Conclusions

The properties of gyrolite are slightly altered by introducing Na^+ ions into its crystal lattice: the main basal reflection *d* spacing increases to 2.324 nm in the X-ray diffraction pattern; the wollastonite formation peak in DSC curve shifts to lower temperatures.

It was found that crystal structure of gyrolite is stable under water vapour pressure at low temperature (in liquid nitrogen, –197 °C) is. It was found that gyrolite is a mesoporous material. Its specific surface area S_{BET} = 143.15 m^2/g, the radius of dominant plate pores r_p = 80–90 Å, the calculated total pore volume ΣV_p = 0.661 cm^3/g. The gyrolite texture changes when Na^+ ions are introduced into the crystal structure: its specific surface area

becomes S_{BET} = 27.24 m^2/g, the radius of dominant cylindric pores r_p = 60–70 Å, the calculated total pore volume ΣV_p = 0.118 cm^3/g.

References

[1] TAYLOR H.F.W., Adv. Cem. Based Mater., 1 (1993), 38.
[2] TAYLOR H.F.W., Cem. Concr. Res., 23 (1993), 995.
[3] ZADOV A.E., N.V.CHUKANOV, ORGANOVA N.I., BELAKOVSKY D.I., FEDOROV A.V., KARTASHOV P.M., KUZMINA O.V., LITZAREV M.A., MOKHOV A.V., LOSKUTOV A.B., FINKO V.I., Proc. Russian Mineralogical Society, 124 (1995), 36.
[4] VIEHLAND D., YUAN L.J., XU Z., CONG X.D., KIRKPATRICK R.J., J. Am. Cer. Soc., 80 (1997), 3012.
[5] SASAKI K., MASUDA T., ISHIDA H., MITSUDA T., J. Am. Cer. Soc., 79 (1996), 1569.
[6] KIRKPATRICK R.J., YARGER J.L., MCMILLAN P.F., YU P., CONG X.D., Adv. Cem. Based Mater., 5 (1997), 93.
[7] YANAGISAWA K., FENG Q., YAMASAKI N., J. Mater. Sci. Lett., 16 (1997), 889.
[8] HEJNY C., ARMBRUSTER T., *Structure modelling and identification of xonotlite polytypes*, [in:] Proc. 6th International Congress on Applied Mineralogy, 2000, pp. 795–797.
[9] SHAW S., HENDERSON C.M.B., CLARK S.M., Chem. Geol., 167 (2000), 129.
[10] KALOUSEK G.L., MITSUDA T., TAYLOR H.F.W., Cem. Concr. Res., 7 (1977), 305.
[11] YANO T., URABE K., IKAWA H., TERAUSHI T., ISHZAWA N., UDAGAWA S., Acta Cryst., 49 (1993), 1555.
[12] GEORGESCU M., TIPAN J., BADANOIU A., CRISAN D., DRAGAN I., Cem. Concr. Comp., 22 (2000), 315.
[13] MARSH R.E., Acta Cryst., 50 (1994), 996.
[14] BALTAKYS K., ŠIAUČIŪNAS R., BALTUŠNIKAS A., Chem. Techn., 1 (2004), 45.
[15] ŠTEVULA L., PETROVIČ J., Cem. Concr. Res., 13 (1983), 684.
[16] ŠIAUČIŪNAS R., BALTAKYS K., Cem. Concr. Res., 34 (2004), 2029.
[17] MIYAKE M., IWAYA M., SUZUKI T., J. Am. Cer. Soc., 73 (1990), 3524.
[18] WINTERS M.A., RICHTER J.D., SAGAR S.L., LEE A.L., LANDEI R.J., Biotechnol. Prog., 19 (2003), 440.
[19] MACKAY A.L., TAYLOR H.F.W., Mineral. Mag., 30 (1953), 80.
[20] CHALMERS R.A., FARMER V.C., HARKER R.I., KELLY S., TAYLOR H.F.W., Mineral. Mag., 33 (1964), 821.
[21] GARD J.A., MITSUDA T., TAYLOR H.F.W., Mineral. Mag., 40 (1975), 325.
[22] LACHOWSKI E.E., MURRAY L.W., TAYLOR H.F.W., Mineral. Mag., 43 (1979), 333.
[23] SHAW S., HENDERSON C.M.B., CLARK S.M., Am. Mineral., 87 (2002), 533.
[24] JAUBERTHIE R., TEMIMI M., LAQUERBE M., Cem. Concr. Res., 26 (1996), 1335.
[25] MERLINO S., Mineral. Mag., 52 (1988), 377.
[26] CHEARY R.W., COELHO A.A., *Programs XFIT and FOURYA, deposited in CCP14 Powder Diffraction Library*, Engineering and Physical Sciences Research Council, Daresbury Laboratory, Warrington, England, (1996) (http://www.ccp14.ac.uk/tutorial/xfit-95/xfit.htm).
[27] GREG S., SING K., *Adsorption, Specific Area, Porosity*, Moscow, Mir, 1984 (in Russian).
[28] ORR C., DALLA VALLE J.M., *Fine Particle Measurements*, MacMillan, New York, 1959.
[29] GARBEV K., PhD Dissertation, Faculty of Geology and Geography, University St. Kliment Ohridski, Sofia, 2004.
[30] NOCUN-WCZELIK W., Cem. Concr. Res., 27 (1997), 83.

Received 20 September 2007
Revised 19 November 2007